CHAPTER 9

9.Mechanistic studies of Bio-active Markers: Synergy, Enzyme kinetics, Fluorescence, Molecular docking & Dynamics

9.1 Two drug combination of gymnemagenin with berberine and palmatine

As noted in the previous chapter, the presence of berberine, palmatine and formation of gymnemagenin in SGF treated composition BARM-GSM prompted us to explore the functional interaction between these bio-active markers. The PL inhibition activity (IC_{50} values) of gymnemagenin, berberine and palmatine were evaluated from the dose-dependent inhibition curve. Gymnemagenin, berberine and palmatine were found to possess an IC_{50} of 7.04 ± 0.32 µM, 28.84 ± 0.45 µM and 37.16 ± 1.21 µM, respectively. Due to the steric bulkiness of berberine and palmatine, their interaction with PL was adversely influenced and hence they showed moderate PL inhibition [1]. Further to understand the functional interatcions, the two-drug combinations were developed by pairing the gymnemagenin with berberine and palmatine (gymnemagenin-berberine: G-B; gymnemagenin-palmatine: G-P). Combination index and isobologram methods (Chapter 4) were used to determine the synergistic interaction amongst the bio-active markers. Gymnemagenin was found to be good synergistic partner with berberine as well as palmatine **(Figure 64)**. Orlistat was used as standard and possesed an IC_{50} value of 0.98 µM.

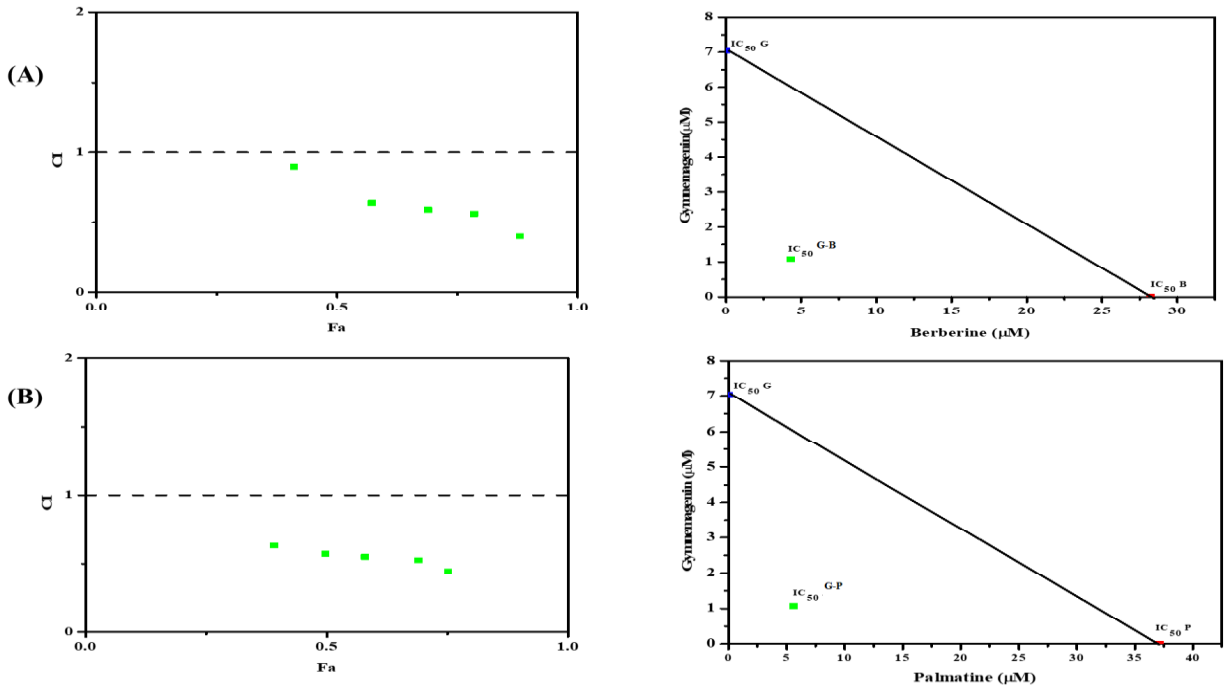

Figure 64: Combination study between (A) gymnemagenin-berberine and (B) gymnemagenin - palmatine

G-B exhibited lower cIC_{50} compared to G-P (**Table 26**). The cIC_{50} of G-B and G-P was found to be 5.42 ± 0.27 and 6.67 ± 1.21 μM, respectively. The amount of berberine and gymnemagenin in G-B was found to be 4.10 and 1.32 μM, respectively. The amount of palmatine and gymnemagenin in G-P was found to be 5.41 μM and 1.26 μM, respectively. These values were used to plot isobologram graph and the plot indicated synergistic interaction as the point lied below the line of additivity **(Figure 64)**.

Table 26: Synergy studies of two drug combination between gymnemagenin, berberine and palmatine

Bio-active markers	**IC_{50}**	**c IC_{50}**	**CI index** (½ IC_{50} Gymnemagenin + ½ IC_{50} berberine/palmatine)	**Effect**
Gymnemagenin	7.04 ± 0.32 μM			
Berberine	28.84 ± 0.45 μM	5.42 ± 0.27 μM	0.56	Synergistic
Palmatine	37.16 ± 1.21 μM	6.67 ± 1.21 μM	0.53	Synergistic

All the values are expressed as mean± S.E.M (n = 3)

9.2 Two drug combination of ECG, EGCG with berberine and palmatine

The presence of ECG, EGCG, berberine and palmatine in SGF treated BARM-TSM composition prompted us to explore the functional interaction between these bio-active markers. Hence, functional interaction between these bio-active markers was further explored by creating the two-drug combinations pairs between ECG/ EGCG with berberine and palmatine (ECG-berberine: ECG-B; EGCG-berberine: EGCG-B; ECG-palmatine: ECG-P; EGCG-palmatine: EGCG-P).

Initially IC_{50} values of ECG, EGCG and berberine, palmatine were obtained from the dose-dependent inhibition curve. The IC_{50} of ECG and EGCG was found to be 12.75 ± 0.26 and 5.84 ± 0.16 μM, respectively. The concentration of ECG/EGCG (0, IC_{50}/8, IC_{50}/4, IC_{50}/2 and IC_{50}) and berberine/palmatine (0, IC_{50}/8, 1/IC_{50}/4, 1/IC_{50}/2 and IC_{50}) were mixed in a constant ratio. Both ECG and EGCG were found to be good synergistic partners with berberine and palmatine **(Figure 65)**.

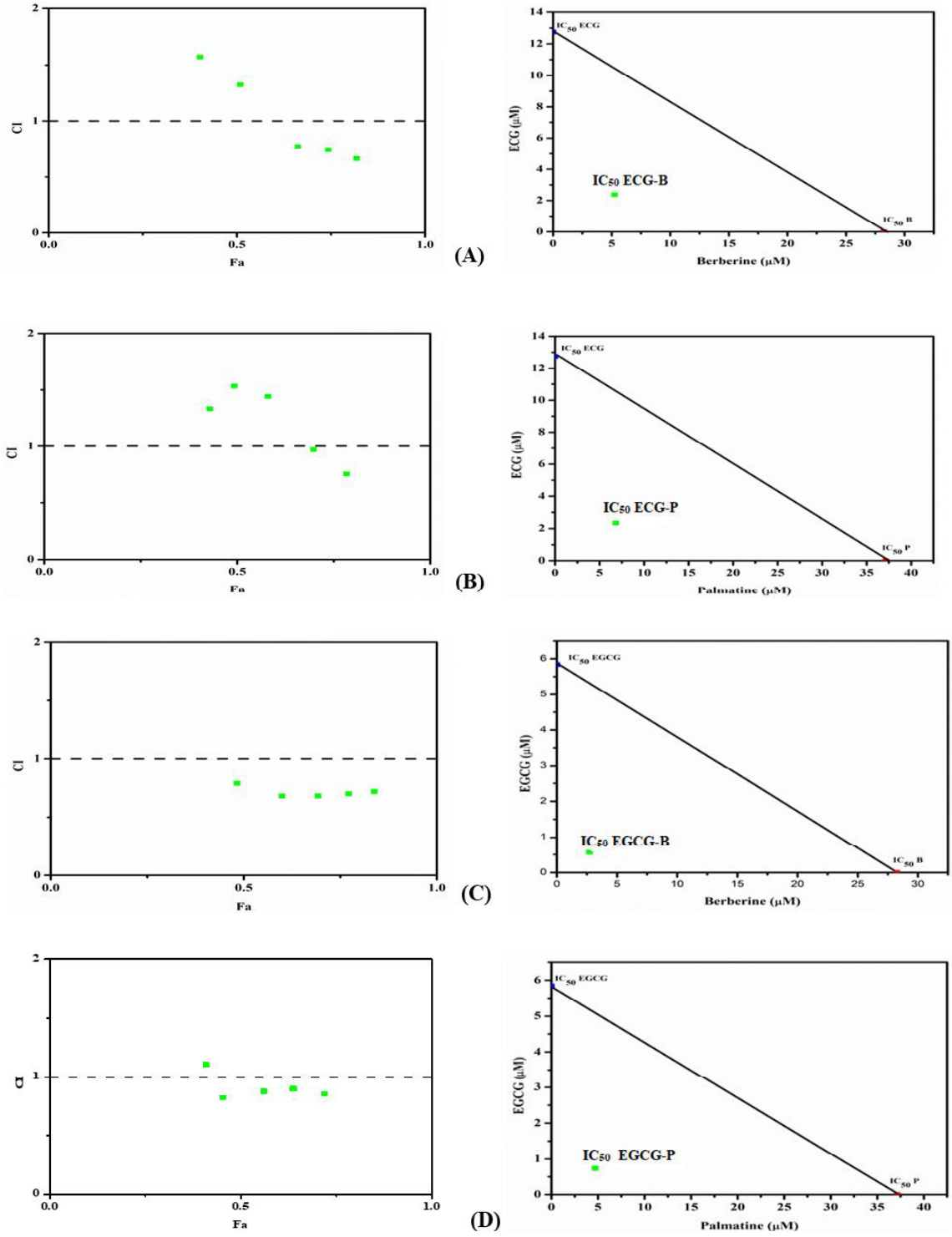

Figure 65: Combination study between (A) ECG-berberine, (B) ECG-palmatine, (C) EGCG-berberine and (D) EGCG-palmatine

The cIC_{50} of the ECG-B, ECG-P, EGCG-B and EGCG-P were found to be 7.62 ± 0.91, 9.17 ± 0.76, 4.26 ± 0.54 and 5.44 ± 0.81 µM, respectively. The amount of berberine and ECG in ECG-B was found to be 4.25 and 3.37 µM, respectively, while palmatine and ECG in ECG-P was found to be 6.02 and 3.15 µM, respectively. The amount of berberine and EGCG in EGCG-B was found to be 3.40 and 0.86 µM, respectively, while palmatine and EGCG in EGCG-P was found to be 4.59 µM and 0.85 µM, respectively (**Table 27**). These values were used to plot isobologram graph and the plot indicated synergistic interactions between all the bio-active markers **(Figure 65)**.

Table 27: Synergy studies of two drug combination between ECG, EGCG, berberine and palmatine

Bio-active markers	**IC_{50}**	**cIC_{50}**	**CI index** (½ IC_{50} ECG + ½ IC_{50} berberine/palmatine)	**Effect**
ECG	12.75 ± 0.26 µM			
Berberine	28.84 ± 0.45 µM	7.62 ± 0.91 µM	0.74	Synergistic
Palmatine	37.16 ± 1.21 µM	9.17± 0.76 µM	0.96	Synergistic
Bio-active markers	**IC_{50}**	**cIC_{50}**	**CI index** (½ IC_{50} EGCG + ½ IC_{50} berberine/palmatine)	**Effect**
EGCG	5.84 ± 0.16 µM			
Berberine	28.84 ± 0.45 µM	4.26 ± 0.54 µM	0.69	Synergistic
Palmatine	37.16 ± 1.21 µM	5.44 ± 0.81 µM	0.89	Synergistic

All the values are expressed as mean± S.E.M (n = 3)

9.3 Two drug combination of ECG, EGCG with gymnemagenin

As noted in the Chapter 8, the presence of ECG, EGCG in GSM-TSM and formation of gymnemagenin in SGF treated compositions prompted us to explore the functional interaction between these bio-active markers. The two-drug combinations were developed by pairing the ECG and EGCG with gymnemagenin (ECG-gymnemagenin and EGCG-gymnemagenin).

The IC_{50} values of gymnemagenin, ECG and EGCG were obtained from the dose-dependent inhibition curve (see sections 9.1 & 9.2). The concentration of ECG/EGCG (0, $IC_{50}/8$, $IC_{50}/4$, $IC_{50}/2$ and IC_{50}) and gymnemagenin (0, $IC_{50}/8$, $1/IC_{50}/4$, $1/IC_{50}/2$ and IC_{50}) were mixed in a

constant ratio. Both ECG and EGCG were found to be good synergistic partners with gymnemagenin **(Figure 66)**.

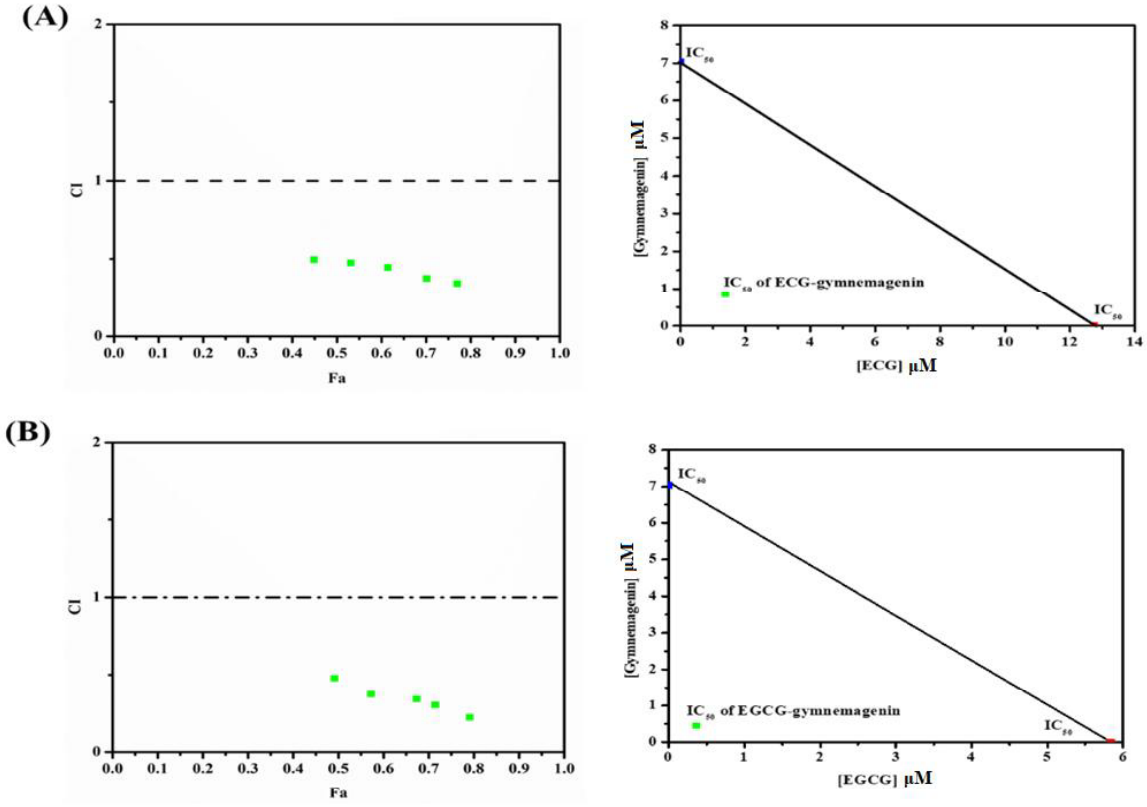

Figure 66: Combination study between (A) ECG-gymnemagenin, and (B) EGCG-gymnemagenin

The cIC_{50} of ECG-gymnemagenin and EGCG-gymnemagenin was found to be 2.15 ± 0.71 and 0.81 ± 1.12 µM, respectively. The amount of ECG and gymnemagenin in ECG-gymnemagenin was found to be 1.19 and 0.96 µM, respectively. The amount of EGCG and gymnemagenin in EGCG-gymnemagenin was found to be 0.67 and 0.14 µM, respectively **(Table 28)**.

Table 28: Synergy studies of two drug combination between ECG, EGCG, and gymnemagenin

Bio-active markers	**IC_{50}**	**cIC_{50}**	**CI index** (½ IC_{50} Gymnemagenin + ½ IC_{50} ECG/EGCG)	**Effect**
Gymnemagenin	7.04 ± 0.32 µM			
ECG	12.75 ± 0.26 µM	2.15 ± 0.71 µM	0.38	Synergistic
EGCG	5.84 ± 0.16 µM	0.81 ± 1.12 µM	0.30	Synergistic

All the values are expressed as mean± S.E.M (n = 3)

9.4 Two drug combination of piperine and pellitorine with alloimperatorin

As noted in the Chapter 8, the presence of alloimperatorin, piperine and pellitorine in AMM-PLM prompted us to explore the functional interactions between these bio-active markers. The two-drug combinations were developed by pairing alloimperatorin with the piperine and pellitorine (alloimperatorin-piperine and alloimperatorin-pellitorine)

The IC_{50} values of alloimperatorin, piperine and pellitorine were obtained from the dose-dependent inhibition curve. The IC_{50} of piperine, pellitorine and alloimperatorin was found to be 20.80 ± 0.60, 18.64 ± 0.78 and 27.75 ± 0.65 µM, respectively. The concentration of piperine/pellitorine (0, IC_{50}/8, IC_{50}/4, IC_{50}/2 and IC_{50}) and alloimperatorin (0, IC_{50}/8, 1/IC_{50}/4, 1/IC_{50}/2 and IC_{50}) were mixed in a constant ratio (**Figure 67)**.

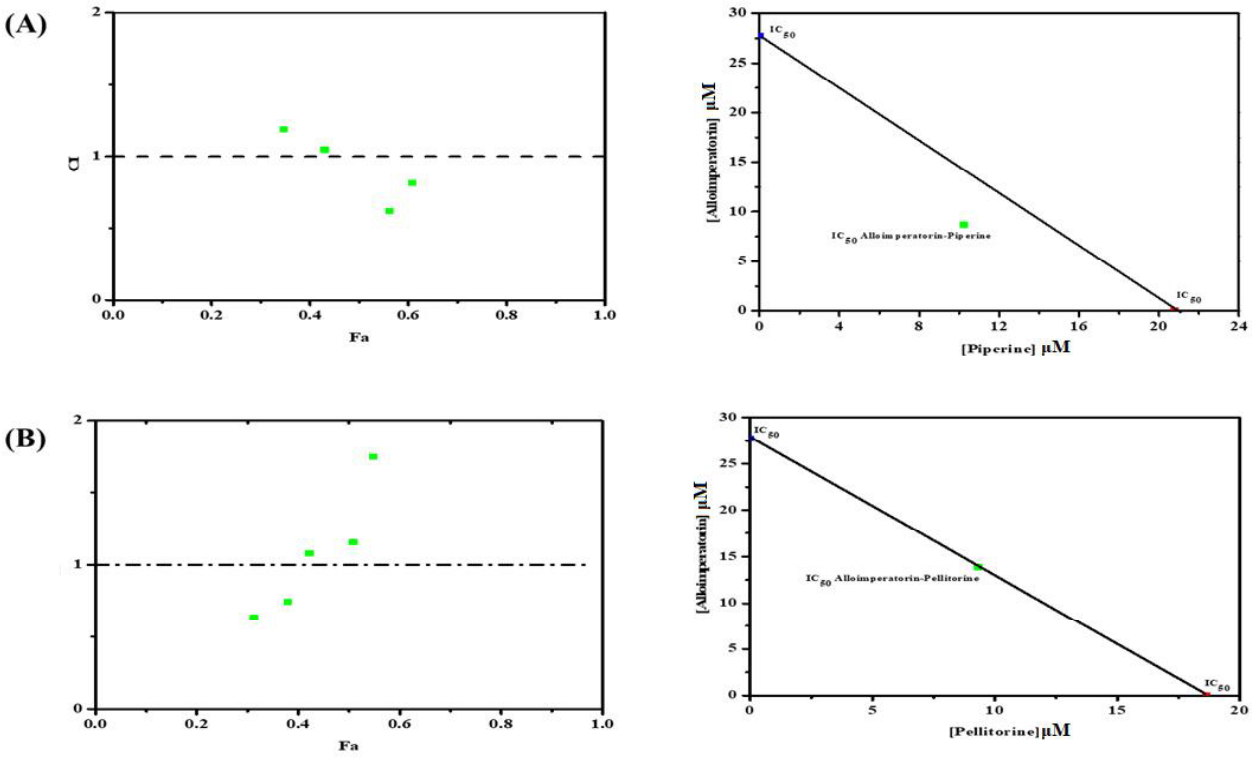

Figure 67: Combination study between (A) alloimperatorin-piperine, and (B) alloimperatorin-pellitorine

The cIC_{50} of alloimperatorin-piperine and alloimperatorin-pellitorine was found to be 18.92 ± 0.34 and 19.88 ± 0.87 µM, respectively. The amount of alloimperatorin and piperine in alloimperatorin-piperine was found to be 10.23 and 8.69 µM, respectively. The amount of

alloimperatorin and pellitorine in alloimperatorin -pellitorine was found to be 13.35 and 6.53 μM, respectively. Alloimperatorin-piperine combination showed synergistic effect, while Alloimperatorin-pellitorine showed anatagonsitic effect. (**Table 29**).

Table 29: Synergy studies of two drug combination between alloimperatorin, piperine and pellitorine

Bio-active markers	**IC_{50}**	**c IC_{50}**	**CI index** (½ IC_{50} Alloimperatorin + ½ IC_{50} Piperine/Pellitorine)	**Effect**
Alloimperatorin	27.75 ± 0.67 μM			
Piperine	20.08 ± 0.60 μM	18.92 ± 0.34 μM	0.62	Synergistic
Pellitorine	18.64 ± 0.78 μM	19.88 ± 0.87 μM	1.07	Antagonistic

All the values are expressed as mean± S.E.M (n = 3)

9.5 Enzyme kinetics

The change in variables affecting the rate of reaction of the enzyme can be defined using enzyme kinetics. There are number of variables affecting the enzyme-substrate reaction such as concentrations of the enzymes, substrates (reactants), products, inhibitors, activators, the pH, temperature, and ionic strength. The enzyme kinetic analysis determines functional characteristic of any enzyme such as the specificities and affinities of the ligands, the order in which substrates bind and products leave, the enzyme species that are intermediates in the overall reaction, the magnitudes of component rate constants, the possible identities of active-site residues, the mode of action of an inhibitory drug, and the behavioral pattern of the enzyme in *in vivo* system.

The rate of catalysis for enzyme rises linearly as substrate concentration ([S]) increases and then a plateau is achieved at higher [S]. The product formation is determined as a function of time for a series of [S]. In each case, the amount of product ([P]) formed increases with time initially, and then a time is reached when there is no net change in the [S] or [P]. The changes in concentration with time is observed until equilibrium has been reached. The factors influencing the rates of reactions is described mathematically using the Michaelis-Menten equation. The Michaelis-Menten equation states that [2]

$$\frac{d[P]}{dt} = v = \frac{[S]V_{max}}{[S] + K_m} \quad \text{....(14)}$$

where, [S] is concentration of substrate, *Vs.* the rate of reaction, V_{max} is the maximal rate that reveals the turnover number of an enzyme (which is the number of substrate molecules converted into product by an enzyme molecule in a unit time when the enzyme is fully saturated with substrate) and K_m is Michaelis-Menten constant. When V is 50%, K_m is always as same as [S]. Hence, K_m is the substrate concentration at which the reaction proceeds at half the maximum rate. There are several ways to determine the K_m, but the most appropriate method is the double reciprocal plot of Lineweaver and Burk (LB). K_m is calculated using the following equation

$$K_m = V_{max} \times \text{slope (m)} \quad \text{....(15)}$$

Similar method have been applied to determine inhibition constant (K_i) for any inhibitor [3]. When inhibitor is added to the reaction, the product formed increases with increase in time, but decreases with increase in concentration of inhibitor ([I]). Using Cheng Prusoff equation K_i is calculated as

$$IC_{50} = K_i\left(1 + \frac{[S]}{K_m}\right) \quad \text{....(16)}$$

When the [S] is high enough, the enzyme will reach the same V_{max} as without inhibitor. However, the K_m of the reaction will be higher. The K_m is represented as apparent K_m (K_m^{app}) [3,4]. Thus enzyme kinetics provides important information about the type of interaction of the inhibitor with the enzyme, that further aids in drug discovery process.

To study the inhibition mode against the PL, enzyme inhibition kinetics analysis of the bio-active markers and Orlistat was performed. The type of inhibition was deduced from the LB plot. The plot was constructed by performing an *in vitro* PL inhibition assay, using various concentrations of the bio-active markers/ Orlistat that were evaluated against the different substrate concentration (25, 50, 100 and 200 µM) [5]. K_i values were deduced from the Cheng-Prusoff equation.

Enzyme kinetics study revealed that berberine and gymnemagenin behaved as a non-competitive inhibitor of PL, while palmatine showed mixed inhibition. In case of non-competitive inhibition, as represented in **Figure 68A** and **C**, the lines converge at the negative X-axis whereas, for mixed inhibition as represented in **Figure 68B**, the line converge in the second quadrant. Both ECG,

EGCG and Orlistat behaved as competitive inhibitor of PL, as the lines converged at the Y-axis of the first quadrant, as represented in **Figure 68D -F**.

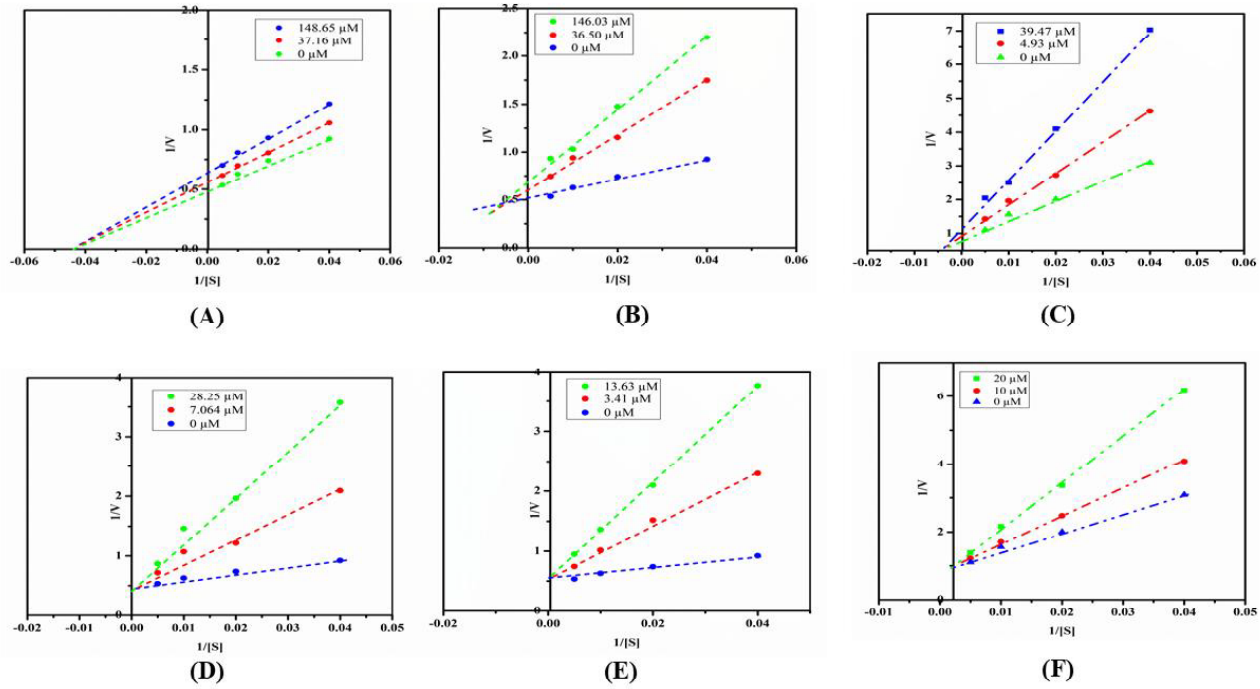

Figure 68: Enzyme kinetics of bio-active markers & Orlistat. (A) Berberine (B) Palmatine (C) Gymnemagenin (D) ECG (E) EGCG and (F) Orlistat

The K_m, V_{max}, and K_i values of the five bio-active markers and Orlistat are tabulated in **Table 30**.

Table 30: K_m, V_{max}, and K_i values of Berberine, Palmatine, ECG, EGCG and Orlistat retrieved from the PL enzyme kinetics

Inhibitors	[I] (µM)	K_m (µM)	V_{max} (µM/min)	K_i (µM)	Type of inhibition
No inhibitor	0	45.10	1.87	0	
Berberine	37.16	45.22	1.62	18.55	Non-competitive
	148.65	45.06	1.43		
Gymnemagenin	4.93	44.97	1.51	3.34	Non-competitive
	39.47	44.91	1.36		
Palmatine	36.50	39.83	1.34	23.91	Mixed
	146.03	37.07	1.07		
ECG	7.06	68.32	1.39	6.09	Competitive
	28.25	80.82	1.15		
EGCG	3.41	61.55	1.34	2.77	Competitive
	13.63	84.80	1.05		
Orlistat	10	53.95	0.91	0.87	Competitive
	20	81.62	0.73		

Piperine and alloimperatorin also showed non-competitive enzyme inhibition (**Figure 69A** and **B**), while pellitorine showed uncompetitive inhibition. In case of uncompetitive inhibition, the lines are parallel to each other as depicted in **Figure 69C**.

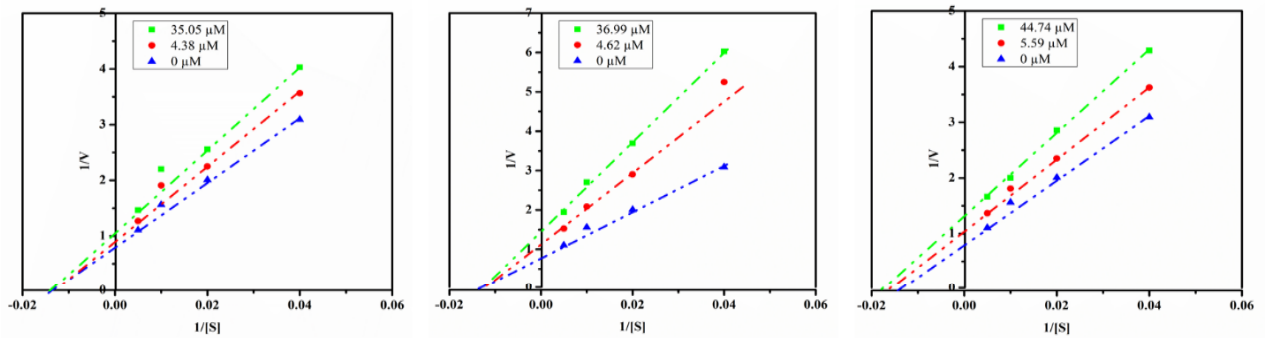

Figure 69: Enzyme kinetics of (A) piperine, (B) alloimperatorin and (C) pellitorine

The K_m, V_{max}, and K_i values of the piperine, alloimperatorin and pellitorine are tabulated in **Table 31**.

Table 31: K_m, V_{max}, and K_i values of piperine, alloimperatorin and pellitorine retrieved from the PL enzyme kinetics

Inhibitors	[I] (µM)	K_m (µM)	V_{max} (µM/min)	K_i (µM)	Type of inhibition
No inhibitor	0	45.10	1.87	0	
Piperine	4.38	45.21	1.56	9.86	Non-competitive
	35.05	45.17	1.35		
Alloimperatorin	4.62	44.89	1.62	13.16	Non-competitive
	36.99	45.01	1.49		
Pellitorine	5.59	37.98	1.23	8.83	Uncompetitive
	44.74	33.77	1.09		

9.6 Binding interactions of bio-active markers with PL using Fluorescence spectroscopy

The interaction between PL and bio-active markers were studied using fluorescence spectroscopy. There are three intrinsic fluorescent groups in any protein that includes residues of phenylalanine (Phe), tyrosine (Tyr), and tryptophan (Trp), amongst which Trp is responsible for emitting major fluorescence. The contribution of Phe to the intrinsic fluorescence of protein is

negligible due to its low absorptivity in addition to a very low quantum yield. Tyr has a similar quantum yield as that of Trp. The indole group of Trp is considered the dominant source of UV absorbance at 280 nm and emission at 350 nm in the proteins [6]. There are seven Trp residues (Trp17, Trp30, Trp86, Trp107, Trp253, Trp338 and Trp403) present in the PL enzyme (**Figure 70**). Trp107 and Trp253 contribute to the major change in fluorescence emission that is triggered by mixed micelles of the inhibitor, as these micelles increase the efficient opening of the lid domain [7,8]. This leads to the conformation changes in PL and is responsible for the peak shift in the fluorescence emission.

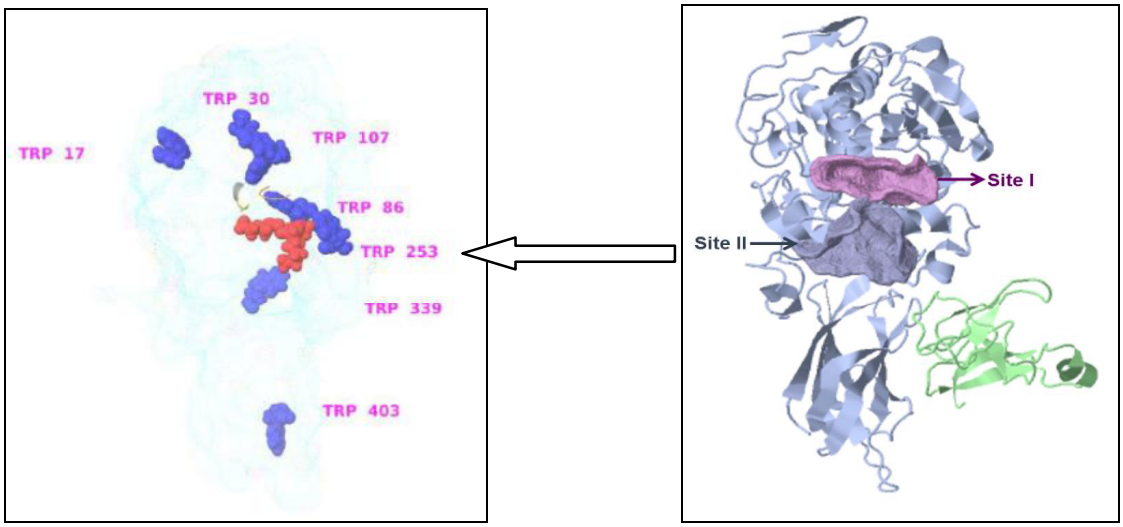

Figure 70: The Trp residues on the surface of PL enzyme

At λ_{ex} of 295nm, PL showed λ_{em} of 347 nm in absence of any bio-active marker. In all cases, bathochromic shift (shift towards longer wavelength) was observed. In case of berberine **(Figure 71A)** and palmatine **(Figure 71B)**, the peak shift of 12 nm and 13 nm was witnessed, while a peak shift of 4 nm, 9 nm and 7 nm was observed for gymnemagenin, ECG and EGCG, respectively (**Figure 71C-E**). Interestingly, piperine displayed 28 nm peak shift with the formation of isosbestic (isoelectric) point at 435 nm (**Figure 71F**). This indicated that the free and bound form of piperine to the PL exists in equilibrium. However, pellitorine being the same type of alkaloid as that of piperine showed a peak shift of only 5 nm with no isosbestic point (**Figure 71G**). Alloimperatorin exhibited a peak shift of 7 nm (**Figure 71H**). This bathochromic shift in all the cases indicated that the Trp residues in this protein are located on the surface of the PL that has contact with solvent molecules [9,10](**Figure 70**). From the earlier reports, Trp-86 and Trp-

107 contribute to the catalytic mechanism of PL. These residues are located on the surface of the catalytic site. Trp 253 is present on the surface of the lid domain (i.e site II) of the active sites. However, if correlated with the results of enzyme kinetics studies, berberine, gymnemagenin, piperine and alloimperatorin were found to bound to other druggable sites nearby to the catalytic region of PL and hence, these molecules behaved as non-competitive inhibitor. Thus, these molecules could be postulated to bind to the site II of PL and interact with Trp 253 that is present in the site II (**Figure 70**) of the lid domain, causing a higher bathochromic shift in the fluorescence of PL. Palmatine exhibited a mixed inhibition of PL, i.e., it behaves in a competitive as well as non-competitive manner. Thus, it might interact with all the three Trp residues (i.e. Trp-86, 107 and 253) to obtain fluorescence emission. On the other hand, ECG and EGCG behaved as competitive inhibitors. Thus, both these bio-active markers might bind to the active site and interacts with Trp-86 and Trp 107, to obtain maximum fluorescence emission with bathochromic shift. From the fluorescence studies it was evident that pellitorine contributed less in the change in fluorescence intensity of PL and a peak shift of 5 nm was observed. Hence, it can be concluded that it formed a complex with PL in uncompetitive manner. Other Trp residues such as Trp17, Trp339, and Trp403 do not contribute significantly to the observed spectral changes as these residues located far away from the active site I and proposed putative site II.

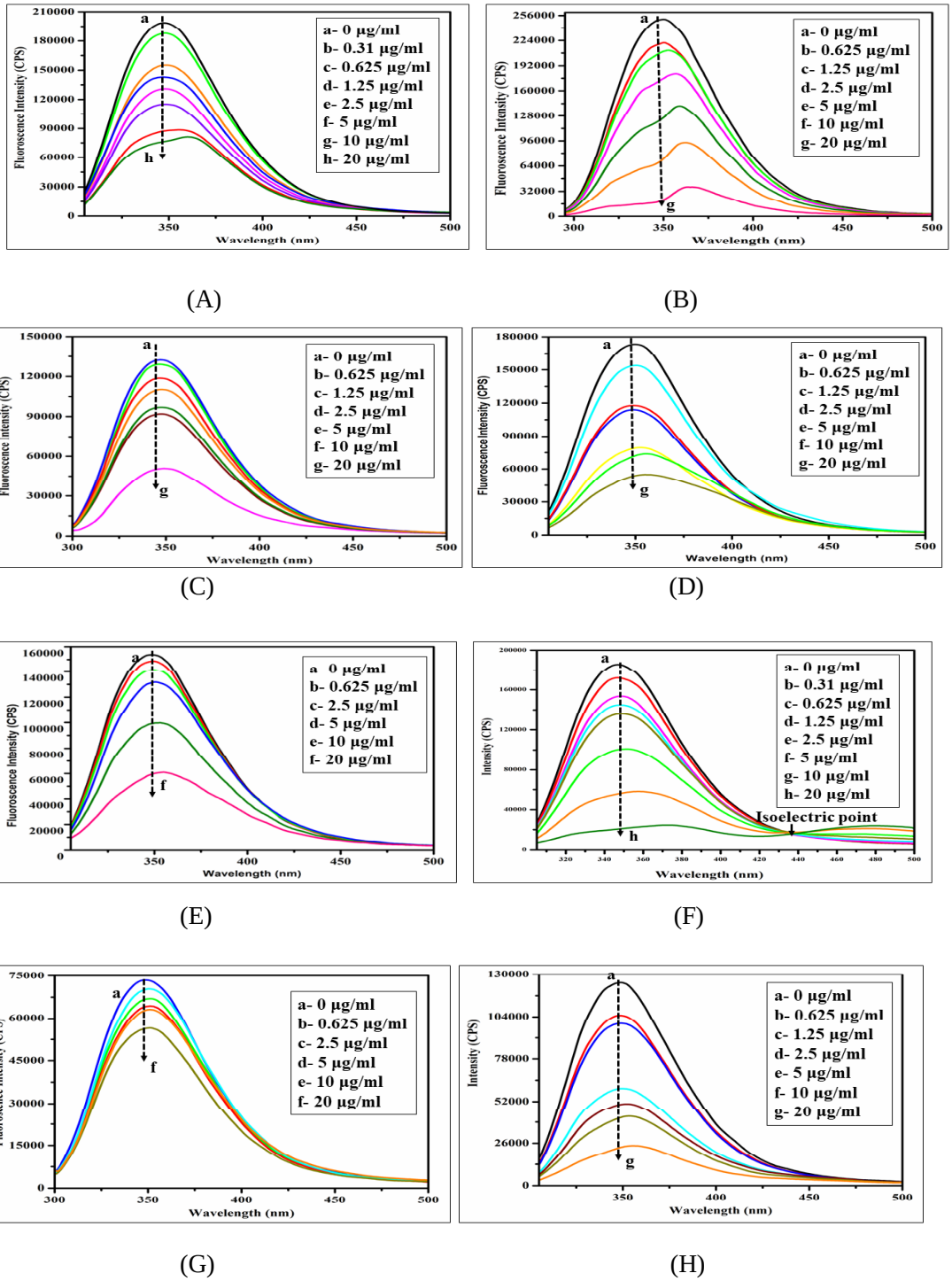

Figure71: Fluorescence study of (A) berberine; (B) palmatine; (C) gymnemagenin; (D) ECG; (E) EGCG; (F) piperine; (G) pellitorine and (H) alloimperatorin

Although, the fluorescence intensity of PL decreases with an increase in the concentration of all these bio-active markers, it revealed the possible interactions with PL. Such observations suggested the quenching mechanism of the fluorescence of PL while interacting with these bio-active molecules. Previous reports suggested that quenching is observed when strong interaction of bio-active molecules with Trp 253 residue occurs in the close conformation of the protein. Strong quenching interaction of bio-active molecules with Trp 107 residues are observed due to fluorescence resonance energy transfer phenomenon [7]. The results obtained imply strong interaction with Trp 253 residues as maximum quenching of PL was observed at higher concentrations of bio-active markers. There are two types of quenching mechanisms involved between the fluorophore (e.g. PL) and the quencher (e.g. bio-active markers) namely dynamic and static quenching. When the collision is encountered between the fluorophore and the quencher, dynamic quenching is observed. Again, when a complex is formed between the fluorophore and quencher from the ground state to the excited state, static quenching is observed. The mechanism of quenching is defined by the Stern-Volmer equation. However, the equation defines either static or dynamic quenching individually, but in many cases, both types of quenching occur simultaneously in the same system. In such cases F_0/F *Vs* [Q] plot illustrates upward curvature and hence, the modified Stern-Volmer equation is used to obtain a linear relationship [11,12]**.**

$$\frac{F_0}{F_0 - F} = \frac{1}{f_a} + \frac{1}{[Q] f_a K_A} \quad \ldots . \textbf{\textit{(17)}}$$

PL suffers both static and dynamic quenching when it interacts these identified bio-active markers, that leads to the utilization of modified Stern-Volmer Plot. The K_A values obtained from the equation are tabulated in **Table 32**. As the K_A value increases the binding capacity of any bio-active markers to PL decreases. To understand the binding capacity, the number of binding sites (n) and binding constant (*K*) were calculated at three different temperatures (298, 303, and 310K) using a double-logarithm regression plot **(Table 32)**. These results signify that the *K* value increases with an increase in temperature that proves the stability of the PL- bio-active markers complex at a higher temperature. Further, 'n' indicate that these ligands employed only one binding site of PL (either site I & II).

Table 32: Quenching constant K_A, the binding constant K, the number of binding sites (n) of PL at different temperature

Sl no	Compound	Temp (K)	K_A (x10^{-4} L/mol)	R^2	K (x10^{-3} L/mol)	R^2	n
1.	Berberine	**298**	2334	0.9935	278.3	0.9725	0.973
		303	1362	0.9814	341.3	0.9904	0.763
		310	950	0.9094	419.2	0.9985	0.722
2.	Palmatine	**298**	1150	0.9952	285.1	0.9853	0.876
		303	1037	0.9767	325.6	0.9784	0.971
		310	811	0.9898	377.4	0.9322	0.798
3.	ECG	**298**	1138	0.9549	182.5	0.9590	0.912
		303	675	0.9888	309.8	0.9567	0.784
		310	657	0.9984	428.9	0.9880	0.861
4.	EGCG	**298**	1984	0.9854	266.4	0.9944	1.021
		303	1192	0.9901	300.1	0.9977	1.050
		310	1097	0.954	395.0	0.9868	0.987
5.	Gymnemagenin	**298**	751.15	0.9224	175.2	0.9765	0.912
		303	481.87	0.9821	298.7	0.9908	1.021
		310	427.54	0.9760	489.22	0.9590	0.880
6.	Alloimperatorin	**298**	746.18	0.9909	308.1	0.9916	1.098
		303	532.77	0.9675	452.3	0.9234	1.129
		310	412.73	0.9732	567.2	0.9876	0.998
7.	Piperine	**298**	422.19	0.9524	206.4	0.9698	0.969
		303	288.17	0.9724	403.4	0.9855	0.872
		310	198.33	0.9816	612.6	0.9921	0.861
8.	Pellitorine	**298**	544.98	0.9654	270.3	0.9987	0.765
		303	387.55	0.9778	490.2	0.9834	0.790
		310	200.43	0.9923	565.5	0.9987	0.876

9.7 Binding interactions of bio-active markers with PL: Thermodynamic calculation

The type of binding force between these bio-active markers and PL was determined by calculating major thermodynamic parameters such as the enthalpy change (ΔH), entropy change ($\Delta S°$) and free energy change ($\Delta G°$) caused due to small temperature fluctuation. These parameters were calculated using the following equation

$$\log K = -\frac{\Delta H°}{RT} + \frac{\Delta S°}{RT} \quad \ldots.(18)$$

where, R denotes gas constant (8.314 J mol^{-1} K^{-1}), and K denotes a binding constant. Further Gibb's free energy was calculated using the equation 9. The values of thermodynamic parameters are listed in **Table 33** that implies that ΔH and ΔG are negative, while ΔS is positive. The negative values of ΔH and positive values of ΔS designate that the binding was enthalpy driven exothermic process. The binding process was due to the van der Waals force and hydrogen bond (favorable non-covalent bonds) formed between the PL and bio-active markers [9]. As the process was

exothermic, the energy of the system was lost and hence the stability of the complex was maintained. The negative value of ΔG indicates that this process was spontaneous [13,14].

Table 33: Thermodynamic parameters of PL at different temperature

Sl no	Compound	Temp (K)	ΔH° (kJ/mol)	ΔG° (kJ/mol)	ΔS° (J/mol K)
1.	Berberine	**298**	-26.21	-66.33	134.62
		303		-67.14	
		310		-67.95	
2.	Palmatine	**298**	-17.94	-49.89	107.19
		303		-50.53	
		310		-51.18	
3.	ECG	**298**	-54.78	-122.54	227.37
		303		-123.90	
		310		-125.26	
4.	EGCG	**298**	-25.14	-64.07	130.60
		303		-64.85	
		310		-65.63	
5.	Gymnemagenin	**298**	-65.76	-144.30	263.59
		303		-145.88	
		310		-147.46	
6.	Alloimperatorin	**298**	-39.13	-92.52	179.15
		303		-93.59	
		310		-94.67	
7.	Piperine	**298**	-69.74	-152.78	278.67
		303		-154.45	
		310		-156.13	
8.	Pellitorine	**298**	-47.44	-108.89	206.24
		303		-110.13	
		310		-111.37	

9.8 Molecular interaction between PL and bio-active markers: Molecular docking & dynamics

Molecular docking and dynamics simulation were used to analyze the interactions between the PL and bio-active markers by directly observing the binding conformation and binding site of the enzyme and the ligand. Molecular docking studies of these bio-active markers were performed using Molegro Virtual Docker 6.0 (CLC bio). The energy minimized structures of these ligands were obtained using MM2 force field in Chemdraw 3D module of ChemBioOffice v12 (PerkinElmer, USA), and docked into the crystal structure of human PL (PDB ID: 1LPB) retrieved from RCSB PDB Data bank. The validation was performed by redocking the co-crystallised ligand (subjected to energy minimization) into the active site of PL. The redocked pose was deviated from the co-crystallised pose by an RMSD of 0.99 Å. The grid resolution was 0.30 Å and radius was 20 Å. The coordinates were X: 7.86; Y: 24.91 and Z: 55.11, respectively.

CHAPTER 9

Molecular dynamics (MD) simulation of bio-active markers in complex with PL was performed using Desmond package (Schoringer LLC). OPLS3e force field was applied during the MD run, and the topology of the ligand was generated. Prior to the initiation of MD, stabilization of the system to 310 K for 50 ns, using canonical NPT and NVT ensembles was done (Chapter 4). The MolDock score of orlistat was found to be -147.442 Kcal/mol and had major interactions with the amino acid residues of the active sites such as Phe 77, Ser 152, Leu153, Tyr 114, Arg 256 and Trp 252. Orlistat formed a stable complex with the enzyme for 100 ns **(Figure 72)**. The interaction of PL with berberine and palmatine were poor due to the rigid structural configuration. The major interaction of berberine with the active site of PL included Phe 77, Tyr 114 and Phe 215, however it didn't show interactions with Ser 152 **(Figure 73A)**. On the other hand, palmatine interacted with Phe 77, Tyr 114, Phe 215, and Arg 256 of the active site of PL **(Figure 73B)**. The MolDock score of berberine and palmatine were found to be -117.546 Kcal/mol and -114.473 Kcal/mol, respectively. The PL-berberine complex was found to be stable for 50 ns, while PL-palmatine was found to be unstable. Gymnemagenin interacted with Phe 77, Tyr 114, Phe 215 and Arg 256 residues of the active site. Interestingly, alkyl interaction with Trp 252 residue was observed (**Figure 73C**). MolDock score was found to be -126.057 Kcal/mol and PL- gymnemagenin complex was found to be stable for 50 ns. ECG **(Figure 73D)** and EGCG **(Figure 73E)** were located in the hydrophobic cavity of PL. ECG and EGCG were found to have major interaction with Phe 77, Try 114, Ser 152, Phe 215, His263 and Arg 256 residues. The MolDock score of ECG and EGCG were found to be -142.542 Kcal/mol and -146.232 Kcal/mol. The two molecules were found to form stable complex with the enzyme for 50 ns. Thus, the results concluded that both these bio-active markers competitively bind to the enzyme and form stable complex with the active site.

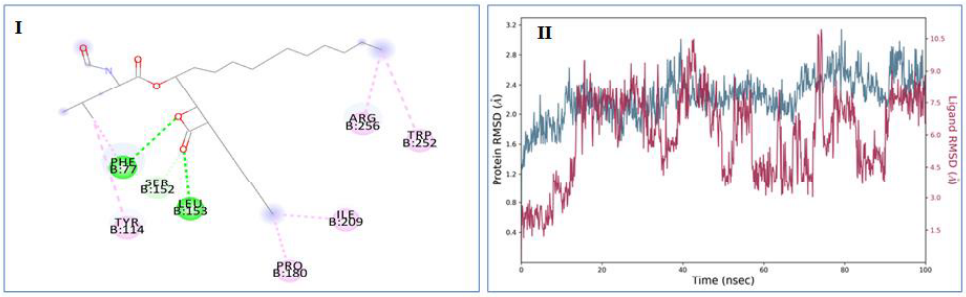

Figure 72: Interaction of Orlistat with PL(I) indicates the best pose obtained from molecular docking; (II) indicates the RMSD plot for 100 ns obtained from Molecular dynamics simulation

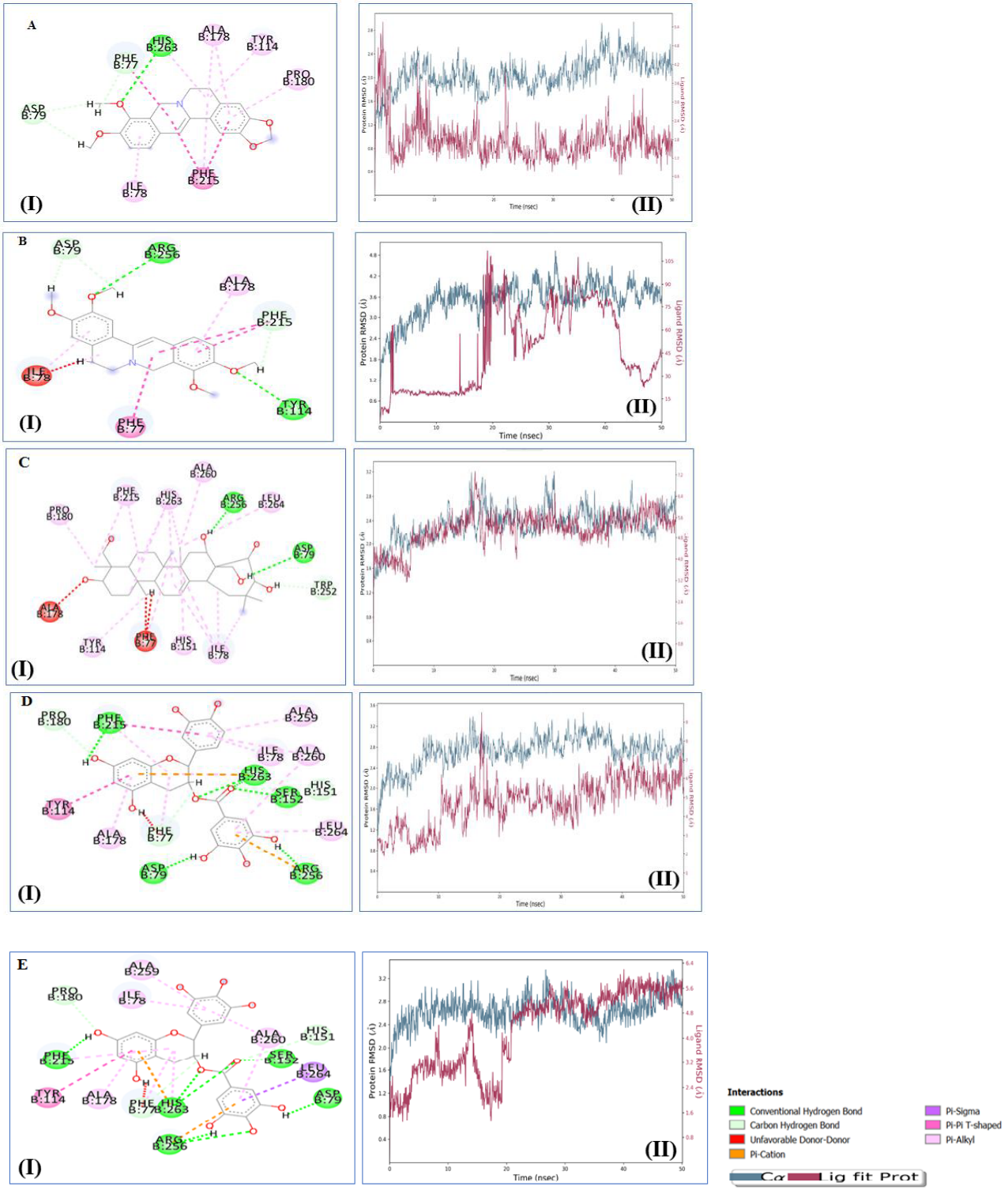

Figure 73: Interaction of bio-active markers with PL(I) indicates the best pose obtained from molecular docking; (II) indicates the RMSD plot for 50 ns obtained from Molecular dynamics simulation for (A) berberine; (B) palmatine; (C) gymnemagenin (D) ECG; (E) EGCG

Docking studies of bio-active markers namely piperine, pellitorine and alloimperatorin were not performed since they showed lower cIC_{50} values [i.e poor synergy or antagonism].

In conclusion, the PL inhibition assay of the phytochemicals were assessed and berberine (IC_{50} = 28.84 ± 0.45 μM), palmatine (IC_{50} =37.16 ± 1.21μM), gymnemagenin (IC_{50} = 7.04 ± 0.32μM), ECG (IC_{50} =12.75 ± 0.26 μM), EGCG (IC_{50} =5.84 ± 0.16 μM), alloimperatorin (IC_{50} =27.75 ± 0.67 μM), piperine (IC_{50} =20.08 ± 0.60 μM) and pellitorine (IC_{50} 18.64 ± 0.78 μM) were found to be bio-active markers. Further these bio-active markers from different extracts were subjected to combination studies. Ten combinations (gymnemagenin-berberine, gymnemagenin-palmatine, ECG-berberine, ECG- palmatine, EGCG- berberine, EGCG- palmatine, gymnemagenin-ECG, gymnemagenin-EGCG, alloimperatorin-piperine and alloimperatorin-pellitorine) were further assessed for PL inhibition. All the above combinations exhibited synergistic effect except alloimperatorin-pellitorine combination that showed antagonistic effect. Kinetics studies revealed that berberine, gymnemagenin, alloimperatorin and piperine exhibited non-competitive inhibition, while ECG and EGCG showed competitive inhibition. Palmatine showed mixed competitive inhibition, while pellitorine behaved as uncompetitive inhibitor. The fluorescence studies revealed that static and dynamic quenching was involved, while these bio-active markers formed a complex with PL. The PL complex with these bio-active markers showed enthalpy driven exothermic process that was due to the formation of van der Waals force and hydrogen bonding. The results obtained from kinetics and fluorescence studies were correlated with *in silico* studies. From the molecular docking and dynamic studies, it can be concluded that ECG and EGCG possessed binding affinity with the active site (site I) of PL, while berberine and gymnemagenin had affinity towards the putative site II. Palmatine behave as mixed inhibitor and therefore it was found to be unstable in molecular dynamics study. Thus we speculate that there bioactives markers when given in combination exhibit synergy due to binding at site I or II for enhanced PL inhibition. However this require further detailed investigation.

References

1. Mohammad M, Al-masri IM, Issa A, *et al.* Inhibition of pancreatic lipase by berberine and dihydroberberine: an investigation by docking simulation and experimental validation. *Medicinal Chemistry Research.* 2013;22(5):2273-2278.

2. Dixon M. The graphical determination of K_m and K_i. *Biochemical Journal*. 1972;129(1):197-202.

3. Kakkar T, Boxenbaum H, Mayersohn M. Estimation of K_i in a competitive enzyme-inhibition model: Comparisons among three methods of data analysis. *Drug Metabolism and Disposition*. 1999;27(6):756-762.

4. Cheng H. The power issue: determination of K_B or K_i from IC_{50}. A closer look at the Cheng-Prusoff equation, the Schild plot and related power equations. *Journal of Pharmacological and Toxicological Methods*. 2001;46:61-71.

5. Sridhar SNC , Mutya S, Paul AT. Bis-indole alkaloids from *Tabernaemontana divaricata* as potent pancreatic lipase inhibitors: molecular modelling studies and experimental validation. *Medicinal Chemistry Research*. 2017;26(6):1268-1278.

6. Teale FW, Weber G. Ultraviolet fluorescence of the aromatic amino acids. *Biochemical Journal*. 1957;65(3):476-482.

7. Bourbon-Freie A, Dub RE, Xiao X, *et al.* Trp-107 and Trp-253 account for the increased steady state fluorescence that accompanies the conformational change in human pancreatic triglyceride lipase induced by tetrahydrolipstatin and bile salt. *Journal of Biological Chemistry*. 2009;284(21):14157-14164.

8 Huo PC, Hu Q, Shu S, *et al*. Design, synthesis and biological evaluation of novel chalcone-like compounds as potent and reversible pancreatic lipase inhibitors. *Bioorganic & Medicinal Chemistry*.2021; 29,1-12

9. Du X, Li Y, Xia Y-L, *et al.* Insights into protein-ligand interactions: Mechanisms, models, and methods. *International Journal of Molecular Science*. 2016;17(2):1-34.

10. Gonçalves R, Mateus N, de Freitas V. Study of the interaction of pancreatic lipase with procyanidins by optical and enzymatic methods. *Journal of Agricultural and Food Chemistry*. 2010;58(22):11901-11906.

11. Wang S, Sun Z, Dong S, *et al.* Molecular interactions between (−)-epigallocatechin gallate analogs and pancreatic lipase. *Plosone*. 2014;9(11):1-10.

12. Papadopoulou A, Green RJ, Frazier RA. Interaction of flavonoids with bovine serum albumin: a fluorescence quenching study. *Journal of Agricultural and Food Chemistry*. 2005;53(1):158-163.

13.Roy S, Nandi RK, Ganai S, *et al.* Binding interaction of phosphorus heterocycles with bovine serum albumin: A biochemical study. *Journal of Pharmaceutical Analysis*. 2017;7(1):19-26.

14.Yu X, Liao Z, Jiang B, *et al*. Spectroscopic analyses on interaction of bovine serum albumin with novel spiro[cyclopropane-pyrrolizin].*Spectrochimia Acta A: Molecular and Biomolecular Spectroscopy*. 2015;137:129-136.